Front. Phys. China (2006) 3: 263—274
DOI 10.1007/s11467-006-0027-7

REVIEW ARTICLE

WU Shi-fa

Review of near-field optical microscopy

Abstract This review has introduced a new near-field optical microscope (NOM)—atomic force microscope combined with photon scanning tunneling microscope (AF / PSTM). During scanning, AF/PSTM could get two optical images of refractive index image and transmissivity image, and two AFM images of topography image and phase image. A reflected near-field optical microscope (AF/RSNOM) has also been developed on AF/PSTM platform. The NOM has been reviewed in this paper and the comparison between AF/PSTM & RSNOM and the commercial A-SNOM & RNOM has also been discussed. The functions of AF/PSTM & RSNOM are much better than A-SNOM & RNOM.

Keywords near-field optical microscope (NOM), atomic force microscope combined with photon scanning tunneling optical microscope (AF/PSTM), SNOM

PACS numbers 07.79.-v, 07.79.Fc, 07.79.Lh

1 Introduction

The resolution of conventional optical microscope is limited by the Raleigh's diffraction limitation (no better than $\lambda/2$). In order to break out the diffraction limitation, Synge [1] proposed an idea of nanometers aperture-scanning near-field optical microscope (A-SNOM) in 1928. O'keefe [2] also made the same creative imagination in 1956. The A-SNOM can not be developed because of the lack of some relational technologies, until the scanning tunneling microscope (STM) was invented by Binning and Rohrer in 1981 [3]. Then, Pohl [4] demonstrated the first A-SNOM experiments on one dimension imaging in 1984. Pohl *et al*. [5], Betzig *et al*. [6], Dürig *et al*. [7] and Muramatsu *et al*. [8] developed the early A-SNOM in 1985—1987. Betzig [9] invented the shear-force mode A-SNOM on constant-distance scanning, where fiber tip is resonant laterally in the near-field of the surface of sample in 1987. A-SNOM with shear-force mode has been commercialized in the world in 1995. Until now, it is the only kind of commercial near-field optical microscope (NOM) whose resolution is beyond the diffraction limitation.

Zenhausern *et al*. [10, 11] demonstrated the apertureless SNOM firstly in 1994—1995, with metal tip and interferometric method and the best optical resolution about 1—2 nm in imaging.

Reddick *et al*. [12] and Courjon [13] developed another NOM named as photon scanning tunneling microscope (PSTM). Ferrel, Warmack and Reddick invented the first PSTM and their patent was authorized in 1991 [14], whose name is brought from (electron) scanning tunneling microscope (STM). The principle and construction of the two kinds of microscopes are the same. Provided $I(Z)$ and $I_e(Z)$ are the information of photon tunneling and electron tunneling respectively, where Z is the gap of tunneling, α, α_e, r and r_e are the constants of tunneling conditions, then [15, 16]:

$$I(Z) = [\alpha \sinh^2(rZ) + 1]^{-1}$$

$$I_e(Z) = [\alpha_e \sinh^2(r_e Z) + 1]^{-1}$$

$I(Z)$ and $I_e(Z)$ are much similar, there fore PSTM is named after STM.

Around 1990 there were some research groups developed the PSTM [17—21]. In China, the first PSTM image of transmission holography grating 1 k pl/mm was achieved in October 1991 beyond the diffraction limitation. And the first PSTM system in China passed the functional examination experiment appraisal in 1993 [22, 23], in which images of over ten types of samples are performed. The lateral resolution of this system is better than 10 nm and the vertical resolution is better than 1nm [24—26].

All of the early PSTM systems in the world utilized single asymmetry laser beam to illuminating sample, and these

WU Shi-fa
Institute of Near-field Optics and Nanotechnology, Department of Physics, Dalian University of Technology,
Dalian 116023, China
E-mail: wsf@dlut.edu.cn

Received July 3, 2006

systems require samples of extremely smooth surfaces to avoid false optical images in PSTM image. In these early PSTM systems using constant high mode and constant height mode the optical and topography images of the samples are always mixed and cannot be separated from each other, and sometimes mixed with image artifacts [27, 28, 16]. These reasons limit the application and industrialization of the early PSTM system.

We applied three invented patents [29—31] and they were granted in 1993 and 1996. These patents provided the methods that can eliminate the false images in PSTM and offer separate the topography image and the optical image. Based on these three invented patents, the first resolution NOM of AF / PSTM (combination of vertical resonance mode AFM with PSTM) was developed and passed the appraisal organized by the experts group of National Ministry of Education in 2002 [32, 33]. The results of functional examination experiments have shown that AF/PSTM prototype is much better than A-SNOM [34]. There are three advantages of this system [35]: (1) It can eliminate the optical false image in PSTM; (2) The optical image and topographic image of sample are separated with AF/PSTM; (3) During scanning two optical images (refractive index image and transmissivity image) and two AFM images (topography and phase) can be obtained. AF/RSNOM (combination of vertical resonance mode AFM with reflected mode-SNOM) has been demonstrated on AF/PSTM platform.

Comparison AF/PSTM and others and the review of NOM are given and discussed in this paper.

2 The super-resolution basic condition and the best choice for *p*- or *s*- polarization

2.1 The conditions of Heisenberg uncertainty principle illustrating the diffraction limit and high resolution [36, 16]

Heisenberg uncertainty principle:

$$\Delta x \cdot \Delta p_x \geq h \tag{1}$$

Here Δx is the uncertainty of emitting photon from sample surface, Δp_x is the uncertainty of x component of this photon momentum p:

$$p = n\,h/\lambda \tag{2}$$

Provided that θ is the aperture angle of imaging system, then

$$p_x = |p| \sin\theta = nh\sin\theta/\lambda \tag{3}$$

The uncertainty Δp_x at photon emitting angle has 2θ, that is from $(-p_x)$ to $(+p_x)$, so

$$\Delta p_x = 2\,p_x \tag{4}$$

For conventional optical microscope (far-field light): only use Propagating light, as a condition of $\theta \leq 90$, with which substituted in expressions (1)—(4), we can get

$$\Delta x \geq \lambda/2\,n\sin\theta \approx \lambda/2 \tag{5}$$

It is more like the Reyleigh diffraction limitation.

Requirement of high resolution in NOM: that is to say $\Delta x \ll \lambda/2$, with which substituted in expressions (1)—(4), we can get

$$p_x \gg |p|,\ \sin\theta \gg 1 \tag{6}$$

This expression means that a component of momentum is much bigger than the absolute value of momentum of photon, so this photon should be the evanescent photon (non-propagating light), and the photon emitting angle θ should be imaginary. The high resolution information of sample only can be carried by evanescent photon and exists in the near-field of the surface of sample.

2.2 *p*-polarization evanescent wave is the best choice for NOM imaging

The *p*-polarization evanescent wave is a longitudinal wave. There is no lateral electronic field, and the lateral on the surface of sample is not influenced. But *s*-polarization evanescent wave is a lateral wave and its electronic field is an axial asymmetry wave, so the lateral electronic field on *s*-polarization orientation should influence the lateral domain much stronger than that of no lateral electronic field orientation.

Figure 1 shows a result of PSTM imaging simulation,

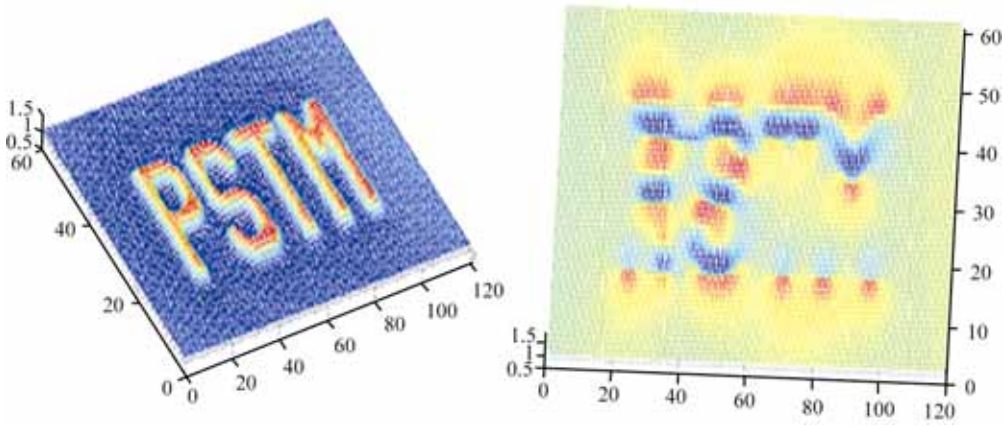

Fig. 1 Simulation of a word "PSTM" of PSTM imaging [35] (left: *p*-polar, right: *s*-polar).

and the sample is a word "PSTM", which is the relief-letters (5 nm × 20 nm on substrate of glass with n: 1.5), with the constant high (CH) scanning-mode (10 nm). The left simulated image "PSTM" is much better than the right one. It means that the best choice for NOM imaging is p- polarization, which emits from the surface of sample.

3 To acquire the pure evanescent wave information of sample is the key in NOM

Generally there are evanescent wave and propagating wave in the near-field of a sample simultaneously, so it is incorrect to say "the near-field light is the evanescent light". The evanescent wave and propagating wave from the surface of sample carry the different resolution information. In near-field the mixed propagating light is not useful but could be harmful to NOM imaging. Therefore, acquiring the pure evanescent wave information of sample is the key in NOM [36].

Now, all of the commercial NOMs included A-SNOM and A-RSNOM work on the shear-force constant height (CH) mode, which can not distinguish evanescent wave with propagating wave. Therefore, the most of commercial NOM images are mixture of the evanescent light and propagating light. The mixed propagating light can decrease the resolution, the contrast and the ratio of signal to noise of NOM image.

Using the characteristics of evanescent wave is the best method to distinguish evanescent wave and propagating wave. The evanescent wave is nearly an exponential attenuation one from the surface of the sample, and propagating wave in near-field is nearly non-attenuation one in $\lambda/2$ distance from the surface of sample.

Three invented patents [29—31] has been used in the system of AF/PSTM or AF/RSNOM. A bi-function bent optical fiber tip is inserted into evanescent wave in near-field of sample, and works on the constant-amplitude scanning imaging mode. As shown in Fig. 2, the tip is actuated by PZT at characteristic resonance frequency, and its amplitude is preset on constant A (near $\sim\lambda/10$).

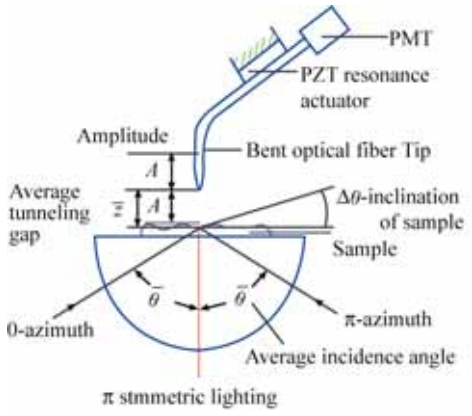

Fig. 2 Schematic of a bi-function bend fiber tip.

The PMT can obtain the photon tunneling information of AF/PSTM or AF/RSNOM. As shown in Fig. 3, $\Delta I = I_{max} - I_{mam}$ is the pure evanescent wave information of the sample, in which any propagating light information has not been mixed. This is because the propagating wave component is nearly a constant in the near-field of $\lambda/4$, which could be eliminated in ΔI.

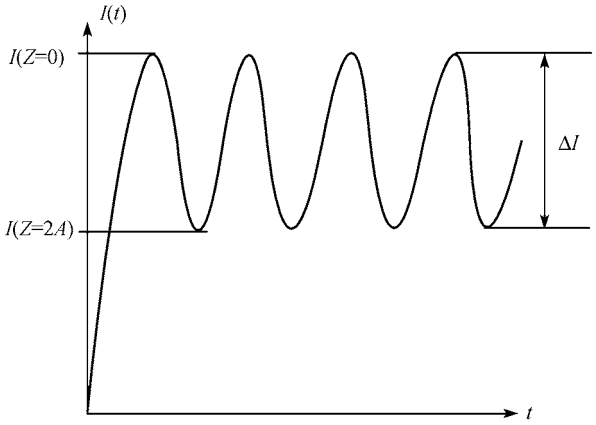

Fig. 3 The waveform of information of PMT (in AF / PSTM or AF/ RSNOM).

For AF/PSTM system the refractive index image ($\Delta n_1(x, y)$) of transmissible sample uses the expression [the same as Eq. (13)] as follows:

$$\Delta n_1(x,y) \propto -[\Delta I(x,y)/I(Z=0)]^2 \tag{7}$$

For AF/RSNOM system the evanescent reflectivity image ($\Delta I_r(x, y)$) and the average reflectivity image ($\bar{I}_r(x,y)$) of a sample use the expressions [37] as follows

$$\Delta I_r(x,y) = [I(x,y,z=0) - I(x,y,z=2A)] \tag{8}$$

$$\bar{I}_r(x,y) = [I(x,y,z=0) + I(x,y,z=2A)]/2 \tag{9}$$

Where $\Delta I_r(x, y)$ is the evanescent reflectivity image of surface of sample in pure evanescent light, and $\bar{I}_r(x,y)$ is the average reflectivity image of the surface sample, in which the evanescent light, propagating light and background light are included.

Figure 4 is the set of AF/RSNOM images of MgF_2 film with hole grating on optical glass surface. $\Delta I_r(x, y)$ is much better than $\bar{I}_r(x,y)$ in resolution, contrast and ratio of signal to noise. $\bar{I}_r(x,y)$ image has been submerged in the background and noise. The reflective indexes of MgF_2 film and optical glass surface are 0.025 and 0.045 respectively. The difference between them is only 0.02. $\Delta I_r(x, y)$ image of AF/RSNOM system has high sensitivity to show the difference of reflective indexes in evanescent wave.

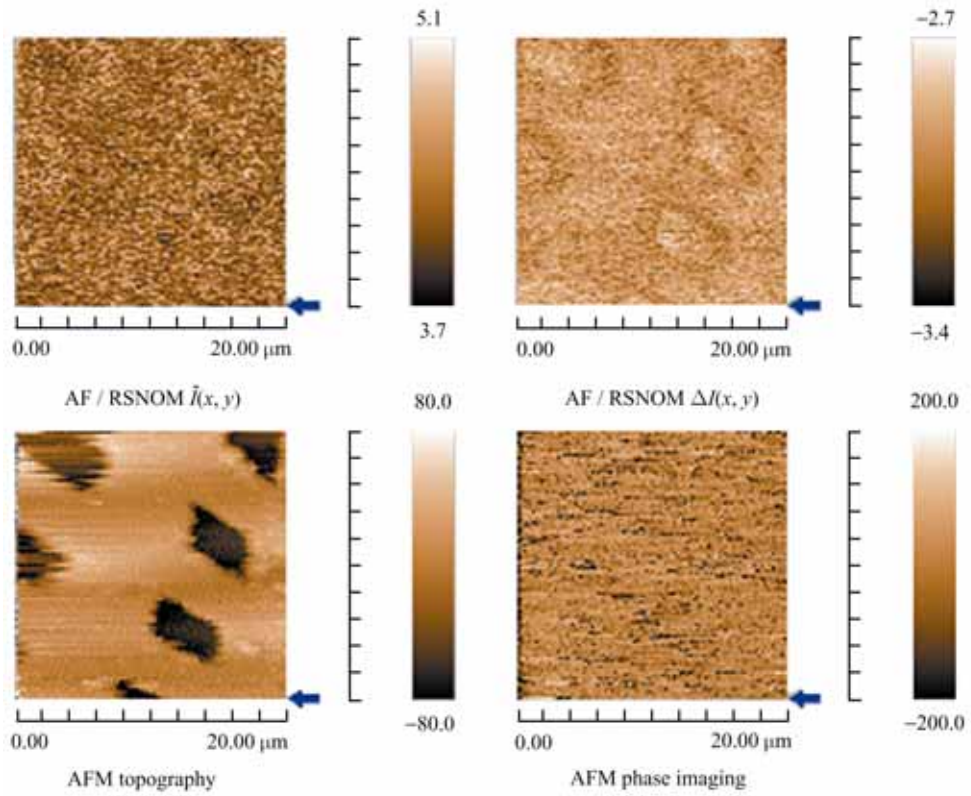

Fig. 4 AF/RSNOM images of MgF_2 film with holes deposited on optical glass surface.

4 The status Quo of NOM and some main problems

Some developed possible configurations of NOM are listed in Table 1, in which there are three kinds: A- SNOM, Scattering-SNOM and PSTM [38].

The two basic conditions to get super resolution imaging are: (1) The illuminating designed to get more evanescent wave emitting from surface of the sample, the evanescent wave on the sample is shown with point line for every configuration of NOM (In table 1); (2) The tip, there are five kinds of probe tips: metalized aperture tip, bare fiber tip, thin metalized apertureless fiber tip, thin metalized pyramid tip, and metal tip.

The most of the NOM configurations in Table 1 have been demonstrated, but only the configuration A_1 and A_3 have been commercialized. Some artifacts faults images will exist in the NOM configuration, such as A_3, A_4, S_3, S_4, S_8 and S_9 in Table 1, particularly in the image of a rough suface, because of the asymmetrical illumination or detection.

The main problems in NOM are:

(i) Some artifacts exist in the image of NOM especially in the asymmetry optical illuminating or detection configuration;

(ii) The optical image of NOM may generally be mixed with some topographic information or thickness information of the sample in constant high or constant intensity scanning mode;

(iii) On the contrast, resolution and ratio of signal to noise of NOM image are degraded by the background scattering especially in bio-samples, except using evanescent wave information ΔI;

(iv) The transmittable efficiency of aperture tip is too low to get high resolution image of A-SNOM.

The main experience and tendency of NOM are:

(i) The combination between NOM and AFM with longitudinal or transversal resonance using bi-function tip;

(ii) Using symmetrical illumination and detection to elimit optical artifacts information;

(iii) Using evanescent wave and abstaining the propagating wave in NOM for improving image:

(iv) Using thin metalized tip or metal tip to improve the resolution and sensitivity of NOM ;

(v) Using metalized tip to enhance focus intensity for modifying film structure or lithography mask in nanometer scale [38];

(vi) Using metalized enhanced tip for spectrum imaging such as Raman scattering or fluorescence imaging [39—42], and so on.

Table 1 The configurations of NOM.

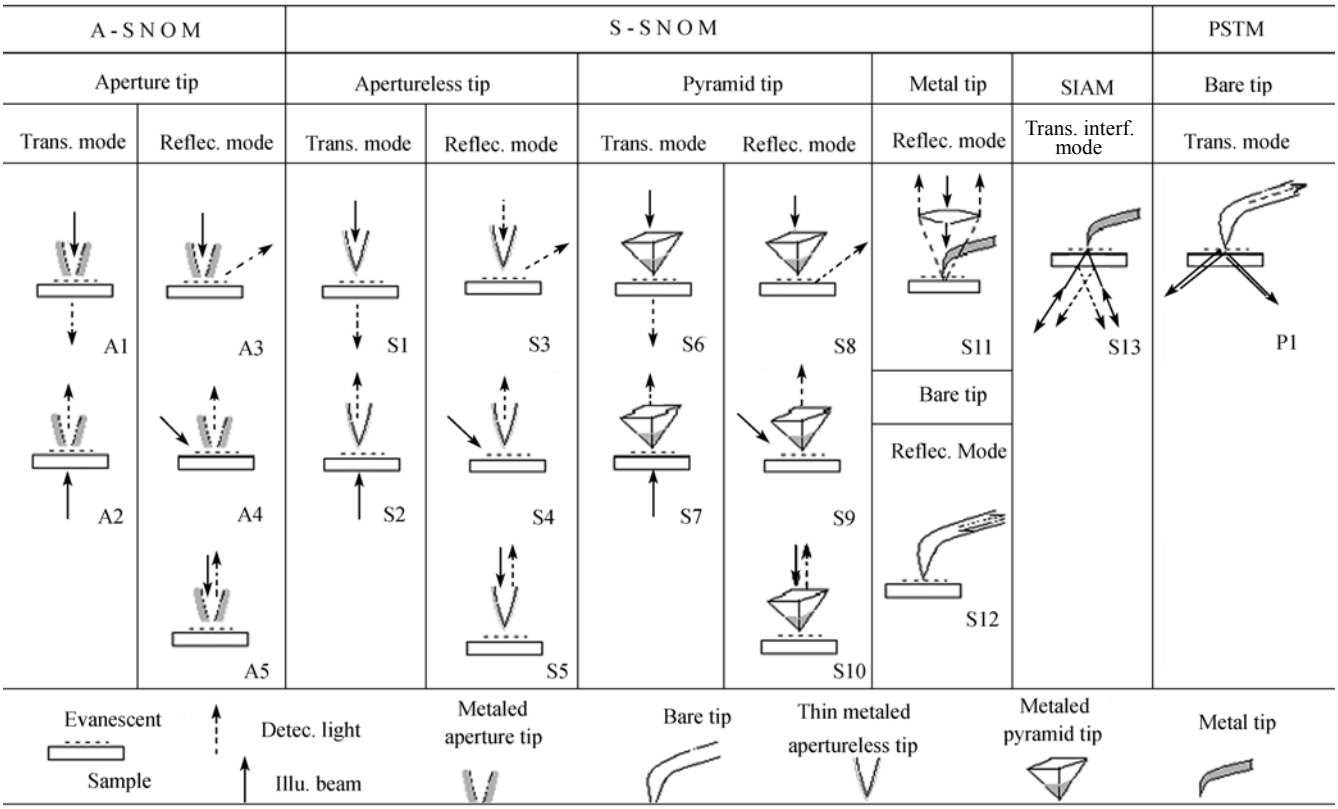

5 The method of separating images and of eliminating false image in AF / PSTM system

The key part of AF/PSTM system is the bi-functional bend optical fiber tip set, as shown in Fig. 2. With it the optical image is separated from topography image in AF/PSTM [31]. The false image with artifacts can be eliminated by using π- symmetry incoherent bi-laser beams and total internal reflected method in AF/PSTM system. Based on numerical simulation and experimentation research the method of eliminating false image with artifacts was confirmed to be effective [29, 31].

5.1 The principle of the method for eliminating artifacts

The photon tunneling information I is a function of Z, n_1 and θ, so

$$I=I(Z, n_1, \theta) \tag{10}$$

As shown in Fig. 5 and Fig. 2, if the angle of inclination of sample surface is $\Delta\theta$, then the incidence angles are $\theta^0 = \theta+\Delta\theta$ for "0"azimuth illumination beam and $\theta^\pi = \theta-\Delta\theta$ for "π" azimuth illumination beam. The differential expressions of (10) are

$$\Delta I^0 = \Delta Z \frac{\partial Z}{\partial n_1}\Delta n_1 \frac{\partial Z}{\partial \theta}\Delta\theta, \text{ for "0" azimuth illumination beam} \tag{11}$$

$$\Delta I^\pi = \Delta Z - \frac{\partial Z}{\partial n_1}\Delta n_1 + \frac{\partial Z}{\partial \theta}\Delta\theta, \text{ for "π" azimuth illumination beam} \tag{12}$$

The "0" azimuth and "π" azimuth beams are isotropic incoherent (p-polarization, equi-intensity and equi-incidence average angle θ, incoherent beam).

Adding (11) and (12) expressions, we can get

$$\Delta n_1 = \left\{\Delta Z - \frac{1}{2}\left[\Delta I^\pi + \Delta I^0\right]\right\} \Big/ \frac{\partial Z}{\partial n_1} \tag{13}$$

By using (13) expression, we have proved that the symmetry illumination can effectively eliminate the optical artifact information contained $\Delta\theta$ items of (11) and (12) expressions. Only a little false image with artifacts may be left in Δn_1. We cannot get Δn_1 image using (13) usual expression, because we have no method to get "$\partial Z/\partial n_1$" yet. The symmetry illumination and detection should be taken to eliminate the optical artifact induced from asymmetrical illumination or detection [43—48].

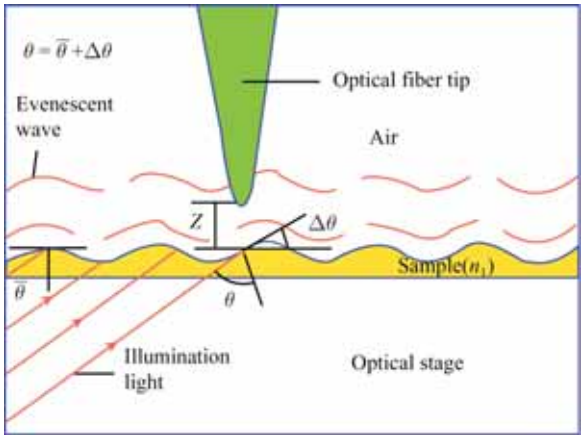

Fig. 5 PSTM sketch of asymmetry illumination.

5.2 The principle of separating images method

The bi-functional bend optical fiber tip, with which the topography image can be separated from the optical image, works with constant amplitude scanning imaging mode at characteristic resonance frequency.

We take the simplest bi-layers (sample and air) model of PSTM imaging, and have got the expressions of the optical refractive index and trasmissivity images of the sample. The sample is illuminated by a pair of π symmetric un-coherent laser beams with a total internal reflection configuration (Fig. 2).

The intensity of the evanescent field at the point of high z above the surface of the sample can be obtained:

$$I(Z)=I(0)\exp\left[-Z\frac{4\pi}{\lambda}(n_1^2\sin^2\bar{\theta}-1)^{1/2}\right] \tag{10}$$

Take the differential equation of (10), setting $\Delta Z=2A$, where A is the amplitude of the tip, then

$$\Delta I=I(\bar{Z}-A)-I(\bar{Z}+A)=I(0)\left[-\frac{4\pi}{\lambda}(n_1^2\sin^2\bar{\theta}-1)^{1/2}(2A)\right] \tag{11}$$

where $I(\bar{Z}-A)$ and $I(\bar{Z}+A)$ are the intensity of the evanescent field at the height $Z=(\bar{Z}-A)$ and height $Z=(\bar{Z}+A)$ above the surface of the sample respectively. ΔI is the value of photon tunneling information of PSTM, which is collected when the bent fiber tip works in the longitudinal resonance. From expression (11) we can get:

$$n_1=K_1-K_2\left[\frac{\Delta I}{I(0)}\right]^2 \tag{12}$$

where $K_1=1/\sin\bar{\theta}$, $K_2=(\lambda/8A\pi)^2/\sin\bar{\theta}$, $\bar{\theta}$ is the average incident angle, A and λ are constants. Then we get the linear relations of the n_1 and $[\Delta I/I(0)]^2$, as following:

$$n_1(x,y)\propto -[\Delta I(x,y)/I(0)]^2 \tag{13}$$

For a four-layer (stage, sample, air and probe) model of PSTM imaging, we have got the results of the numerical simulation that is shown by the expression (13) is also available [48]. When $T(x, y)$ is the transmissivity image of a transparent sample, $I(0)=I(x, y, Z=0)$ is the photon tunneling information image of PSTM at $Z = 0$. Setting the average intensity of the incident light is a constant (I_0), $I(0) = T(x, y, Z=0)\ I_0$, then the transmissivity image of sample is as follow

$$T(x,y)=I(x,y,Z=0)/I_0 \tag{14}$$

$$T(x,y)\propto I(x,y,Z=0) \tag{15}$$

According to expressions (13) and (15), if we have separated the $\Delta I(x, y)$ and $I(x, y, Z = 0)$ from the information of the photon tunneling of AF/PSTM scanning, the reflective index and transmissivity images of the sample can be obtained. Therefore, PSTM unit is designed to separate the ΔI and $I(0)$ from the information of the photon tunneling using outputted by photon multiplier tube (PMT) and reveal $n_1(x, y,)$ and $T(x, y)$ by real time calculation.

6 The prototype framework and the photo of configuration of AF/ PSTM

The AF/PSTM prototype is made up of a main microscope below a binocular stereomicroscope, the control system, photoelectric multiplier tube, preamplifier and computer. The amplification of the binocular stereomicroscope, PSTM and AFM are about 7×–270×, thousands to ten thousands, and hundreds of thousands respectively. The structure framework and the photograph of the AF/PSTM prototype are shown in Fig. 6 and Fig. 7 respectively. The AF/PSTM works in constant-amplitude resonance mode, which can eliminate the false optical image with artifacts and obtain the refractive index image $\Delta n_1(x, y)$, transmisivity image $T(x, y)$, the topography image $\Delta Z_0(x, y)$ and phase image $\Delta P(x, y)$ of the sample. If the surface of the sample is uneven, the optical lever of AFM detect the topographic image, and collect the difference of the phase image between the signal of the optical levers and the resonance actuator signal.

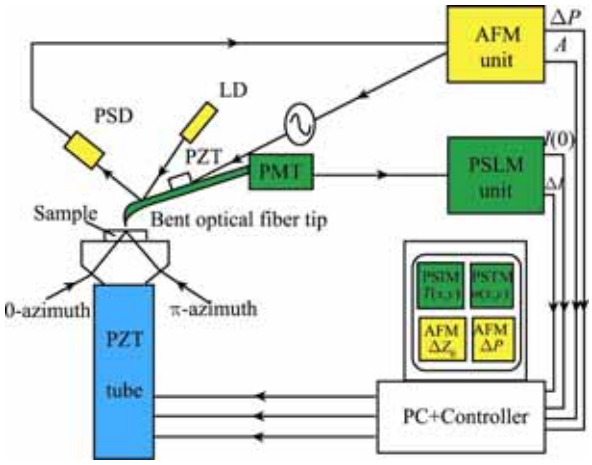

Fig. 6 AF / PSTM block diagram.

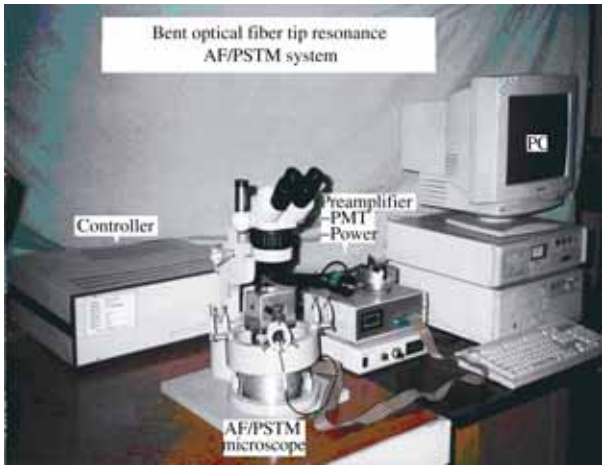

Fig. 7 Photograph of AF/PSTM.

7 Some experimental results of AF/ PSTM

In order to examine the functions of the AF/PSTM, we prepared some samples whose parameters had been known. There are two samples: a 2.4 k pl/mm replication transmission grating and an MgF_2 film with holes covered on optical glass plate. Some selected images of AF/PSTM are presented.

7.1 A 2.4 k pl/mm replication transmission grating

The topography of this grating with known refractive index is made of resin.

Figure 8 is a set of AF/PSTM images of 2.4 k pl/mm replication transmission grating. There is clearly grating structure in the topography image, transmittivity image and phase image. The material of replication grating is resin with equal refractive index, so there is no clear grating image in the refractive index image. Transmittivity image shows that there is a fixed vibration frequency in knife trace images during the carving process, which has not been discovered in the past. Therefore, AF/PSTM provides a new detecting method for the nanometer fabricating process.

7.2 A MgF_2 film with 2D array holes deposited on optical glass substrate

This sample has two different media, MgF_2 (the refractive index is 1.38) and optical glass plate (the refractive index of is 1.55).

Figure 8 is a set of AF/PSTM images of MgF_2 film with holes on optical glass plate. There are not only the clear grating images in the topography image, transmittivity image and gradient image, but also in refractive index image. The bottom of the holes of MgF_2 film is the optical glass. The refractive index of the optical glass substrate is 1.55 and the refractive index of MgF_2 film is 1.38. The refractive index image of the optical glass substrate is darker than that of MgF_2 film which is in good agreement with the minus in Eq. (13).

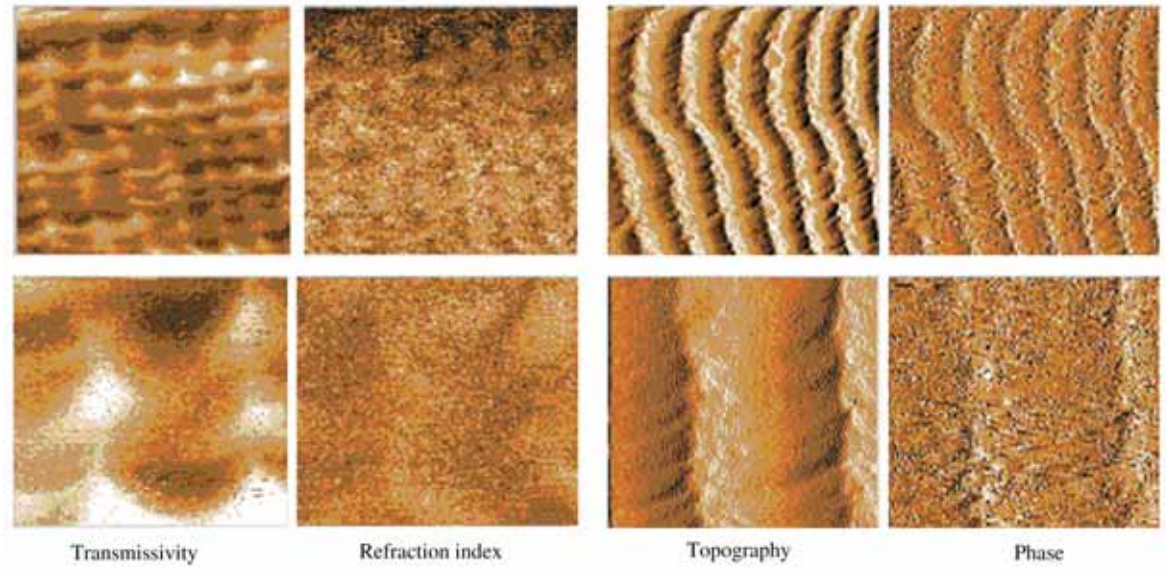

Fig. 8 AF/PSTM images of 2.4 k pl / mm copy grating (up: 2.75×2.75 μm^2, lower: 0.82×0.82 μm^2).

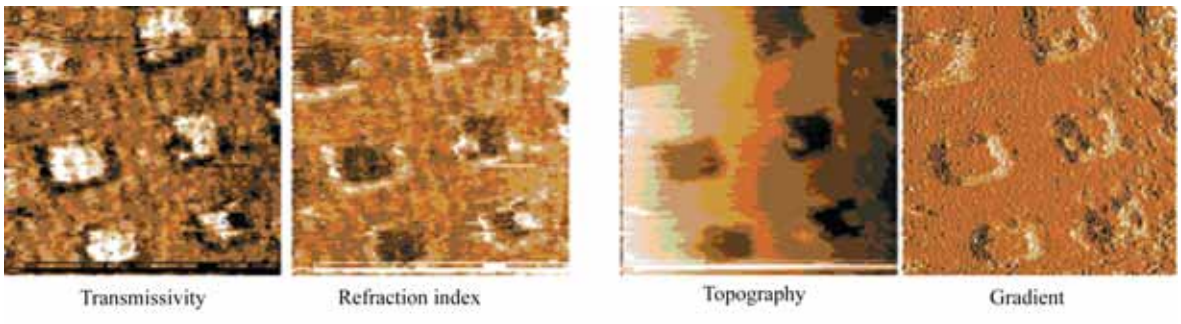

Fig. 9 AF / PSTM images of MgF_2 film with holes on glass16×16 μm^2.

7.3 A holographic transparent grating

Figure 10 is a set of AF/PSTM images of holographic transparent grating. The four images show that the AF/PSTM is more powerful than anyone of AFM or PSTM and is much better than A-SNOM. The A-SNOM only can get the transmisivity image but cannot get the refractive index image, which is important in optical image of sample. There is a convexity speckle (bright) in the topography image. The phase image does not seem to any information but noise. It means that even at the position of the convexity speckle the holographic film latex be covered fully. The transmissivity image shows that there is a translucent foreign particle at the position of convexity speckle, that influences the trans missivity. One would ask where the foreign particle is, is it on the top of the holographic film latex, in it , or below it? Scanning probe microscope (SPM) would not be able to answer this question but AF/PSTM can. Comparison and analysis of the four images in Fig.10 clearly indicate that the foreign particle is below the film latex and on the flat substrate of glass plate. That can be explained as follows. Though the translucent foreign particle influences the transmisivity image, it does not affect the refractive index detection because it is not shown in the refractive index image, thus it can be the result of the silver particles deposited in the holographic film latex that forms the grating.

There is a special advantage of the imaging of AF/PSTM on refractive index image. The non-uniform illumination does not influence the refractive index imaging of AF / PSTM, so the intact gating image can be seen in the refractive index image. This is because the cause of $n_1(x, y)$ is only related to the relations of $I(x, y)$.

7.4 The erythrocyte membrane

Figure 11 is a set of AF/PSTM images of erythrocyte mem-

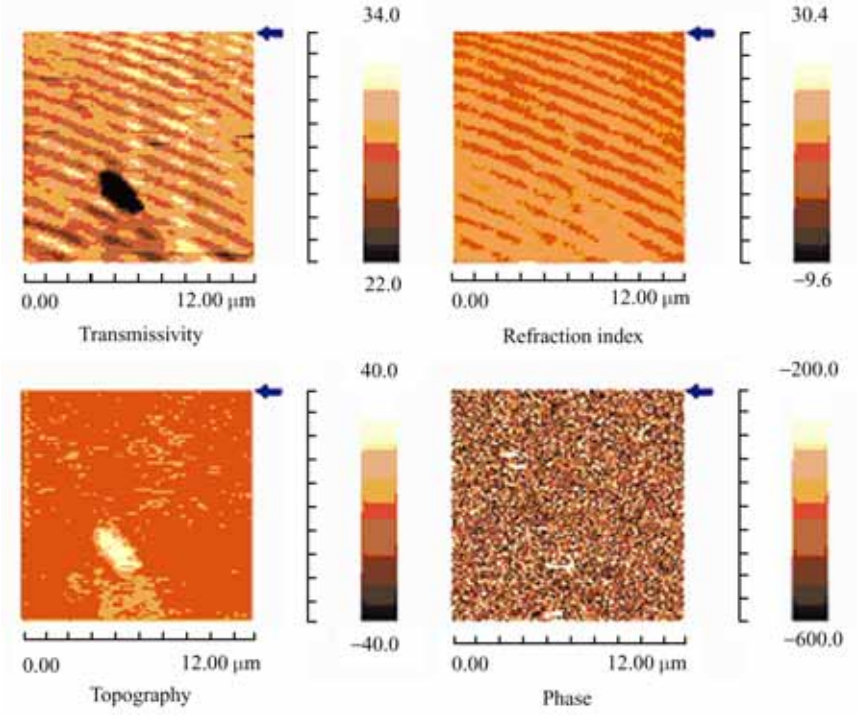

Fig. 10 AF/ PSTM images of holograph grating(1 k pl/mm).

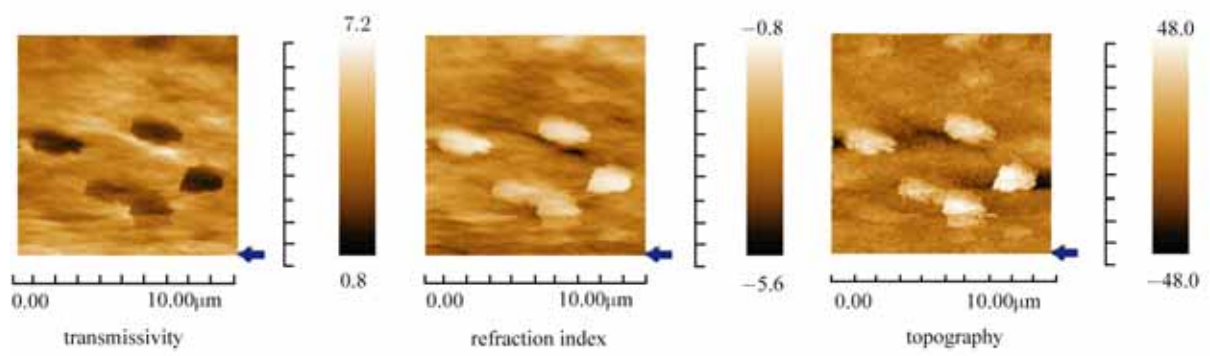

Fig. 11 AF / PSTM images of erythrocyte membrane fragments.

brane after cleaning the hemoglobin. The erythrocyte is broken by contrary filter method to get the erythrocyte membrane fragments. After cleaning the hemoglobin, we got the transmissivity image, reflective in- dex image and AFM topography image of the erythrocyte membrane fragments.

Figure 11 shows that the sensitivity of refraction index imaging of AF / PSTM is bout 5 nm thickness of bio-membrane being detected.

8 Numerical simulation of PSTM

8.1 Simulation of the PSTM tunneling

The finite difference time domain (FDTD) technique has been proved to be fruitful for solving electromagnetic field problem in visible frequency. However, the boundary condition is complex for nanometer scale resolution in PSTM. We proposed equivalent incident wave method [49] and three-wave method to solve the problem of the incident field setting and developed the PSTM-FDTD software. The phenomena of photon tunneling in PSTM [50] is demonstrated, and a separation of the refractive index and topography in STM is simulated and verified with experiments [51]. The boundary condition of the tunneling phenomena simulation shows in Fig. 12, the tunneling phenomena is shown in Fig. 13.

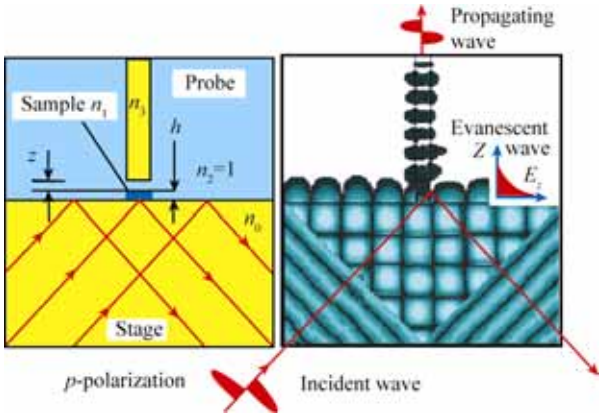

Fig. 12 The boundary condition of PSTM tunneling.

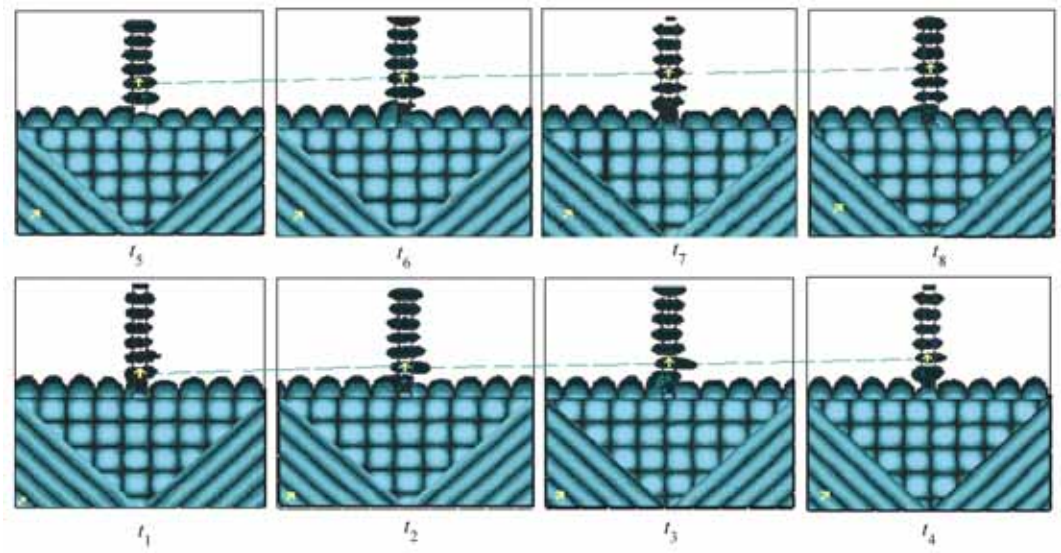

Fig. 13 The simulation of the phenomena of photon tunneling in PSTM.

The incident wave is the parallel *p*-polarization beam in stage. An evanescent wave is on the surface of sample. The propagating wave translates in the probe.

Figure 13 shows the simulation of the photon tunneling phenomena in PSTM with the time t_1–t_8.

8.2 Vertification of the refractive index image expression of AF / PSTM

PSTM-FDTD numerical simulation verifies the refractive index image expression (13) of AF/PSTM. Figure14 shows a simulation result with PSTM-FDTD, that is the relationship between $[\Delta I/I(0)]^2$ and the refractive index $n_1(x, y)$ of the sample is near linear in the $n_1(x, y)$ scale 1.2—2.8 (the size of sample is 200 nm×100 nm×50 nm, $\lambda = 632.8$ nm, and ΔZ is double amplitude of the fiber tip).

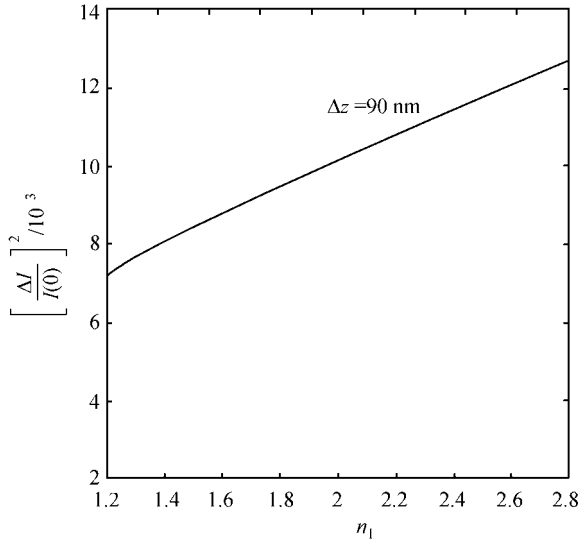

Fig. 14 $n_1 - \left[\frac{\Delta I}{I(0)}\right]^2$ simulation with PSTM-FDTD.

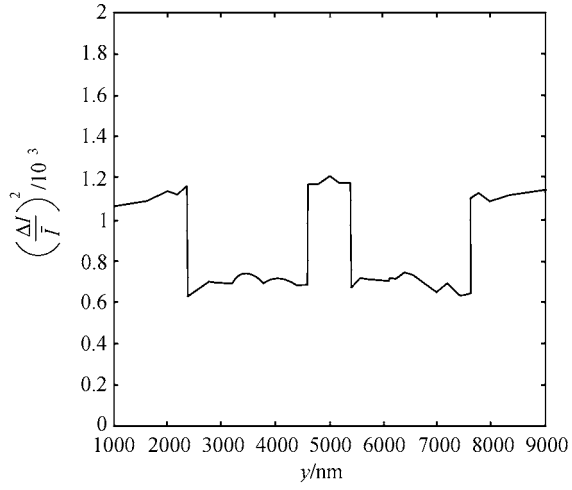

Fig. 15 Simulated image as same as in Fig.7 (MgF_2 film).

We also verify the results of the numerical simulation with the experimental image of AF/PSTM. The sample is the MgF_2 film with holes on glass (As shown in Fig. 9 AF/PSTM images). The conditions of FDTD numerical simulation are as same as the experimental ones. As shown in Fig. 9 and Fig. 15, the simulated cross section in Fig. 15 of sample is as same as the refractive index image of AF/PSTM in Fig. 9.

9 Acomparison between the AF/PSTM & RSNOM and the commercial A-SNON & RSNOM

The comparison between AF/PSTM & RSNOM and commercial A-SNON & RSNOM are shown in Table 2. AF/PSTM & RSNOM has not been commercialized, but their function may be much better than that of commercial A-SNOM & RSNOM. AF/RSNOM could get unique ΔI image but A-RSNOM could not because that A-RSNOM works with shear-force mode [52].

A-RSNOM cannot get evanescent light reflected image $\Delta I_r(x, y)$ but can get a mixed image of evanescent and propagating waves, which are always submerged in background.

Table 2 shows the comparison of AF/PSTM with commercial A-SNOM. The former could get the unique $n_1(x, y)$ image of AF/PSTM while A-SNOM cannot, the latter can only get transmissivity image like $T(x, y)$ of AF/PSTM.

PSTM has 1—2 orders better than A-SONM in resolution, contrast and transmitting effect. The best experimental result of PSTM we got is the value of the full-width at half-maximum 2.8 nm [53], and the routine resolution of PSTM is 10—20 nm. The resolution of PSTM is decided by the size of the center of the bare fiber tip, and the resolution of the A-SNOM is approximately given by the size of the metal aperture wall. In A-SNOM, the output from optical fiber tip decreases rapidly as the aperture diameter reduces, and the reduced aperture diameter is restricted by the limited sensitivity requirement of the systems. The routine resolution of a general A-SNOM is about 50—100 nm.

In NOM the high resolution only depends on evanescent field. It is important that as high as possible of the transform efficiency from illuminating light to evanescent light on the sample surface is as high as possible. The best one is the total internal reflective mode. Nearly 100 % illuminating light can transform to evanescent light in PSTM. In A-SNOM the evanescent light is very weak and almost leaked as forbidden light, which will be not used for imaging. The light permeated the sample is almost propagating light, only a little evanescent light scattered from the aperture wall, which carries the sample's information beyond the diffraction limitation. Most imaging light of A-SNOM is propagating light, so the contrast of A-SNOM is lower than that of PSTM.

Table 2 A comparison of AF / PSTM & RSNOM with commercial one.

Comparison	Our's AF / PSTM & RSNOM	Commercial A-SNON & RSNOM
Mode	Vertically resonance mode	Shear-force mode
Resolution, contrast & ratio of signal to noise	High	Lower
Applicability	Live bio-soft sample	Died bio-solidify sample
Transmitting parameters	Refractive & transmissivity index	Only transmissivity index
Reflecting system's parameters	Lighting & detecting symmetry	RSNOM detecting asymmetry
Artifacts	No artifacts	RSNOM may have artifacts

10 Conclusion and outlook

This paper has introduced a new near-field optical microscope (NOM)-atomic force microscope combined with photon scanning tunneling microscope (AF/PSTM) with bend optical fiber tip actuated with vertical resonance. During scanning AF/PSTM can get the refractive index image, the trasmissivity image, the topography image and phase image. A reflected near-field optical microscope (AF / RSNOM) has been developed on the AF/PSTM platform.

The NOM has been reviewed in this paper and the comparison between AF/PSTM & RSNOM and the commercial A-SNOM & RNOM has also been discussed. The functions of AF/PSTM & RSNOM are much better than A-SNOM & RNOM, so the industrialization of AF/PSTM will be prospered.

Acknowledgements This work was supported by the Fundamental Research Program (Pre-research No. 2004 CCA 03700) and Instrument Program (No. GN-99-15) of the National Ministry of Science and Technology China, and the National Natural Science Foundation (Grant No. 60007011).

References

1. Synge E. H., A suggested method for extending microscopic resolution into ultra-microscopic resolution, Phil Mag., 1926, 6: 356—362
2. O'keefe J. A., Resolving power of visible light, Opt. Soc. Am., 1956, 46(5): 359
3. Binning G. and Rohrer H., Scanning Tunneling Microscopy, Helv. Phys. Acta., 1982, 55: 726—735
4. Phol D. W., Denk W., and Lanz M., Optical stethoscopy image recording with resolution $\lambda/20$,Appl. Phys. Lett., 1984, 44: 651—653
5. Pohl D. W., Fischer U. Ch., and Düring U., Optical stethoscopy: image with $\lambda/20$, Proc. SPIE Micron and submicron integrated circuir metrology, 1985, 565: 56—61
6. Betzig E., Harootunian A, et al., Near-field Scanning Optical Microscopy, Biophys J., 1986, 49: 269—279
7. Düring U., Pohl D. W., and Rohner F., Near-field optical scanning microscopy, J. Appl. Phys., 1986, 59: 3318—3327
8. Muramatsu H., Chiba N., Ataka T., et al., Scanning Near-field Optic / Atomic Force Microscopy, Ultramicroscopy,1995, 57: 141—146
9. Betzig E., Finn P. L., and Weiner T. S., Combined shear force and near-field scanning optical microscopy, Appl. Phys. Lett., 1992, 60, 2484—2486
10. Zenhausern F., O'Boyle M.P., et al., Apertureless Near-field Optical Microscopy, Appl. Phys. Lett. 1994, 65 (13): 1623—1625
11. Zenhausern F., Martin Y., and Wickramasinghe, Scanning Interferometric Apertureless Microscopy: OpticalImaging at 10 Angstron Resolution. Science, 1995, 269: 1083—1085
12. Reddick R., Warmack R., and Ferrell T., New form of scanning optical microscopy, Phys. Rev. B, 1989, 39 (1): 767—770
13. Courjon D., Sarayeddine K., and Spajer M., Scanning tunneling optical microscopy, Opt. Commun. 1989, 71: 23—28
14. United States Patent Number:5,018,865. 1991-05-28
15. Zhu S., Yu A. W., et al., Frustrated total internal reflection: A demonstration and review, Am. J. Phys., 1986, 54(7): 601—607
16. Wu Shifa, Morden imaging technology and image processing, Beijing: the publishing House of National Defense Industry of China, ISBN 7-118-0165-4, 1997: 494 (in Chinese)
17. Reddick R. C., Warmack R. J., and Ferrel T. L., Photon scanning tunneling microscopy, Review of Science Instrument, 1990, 61: 3669—3677
18. Vigourcux J. M., Girard C., et al., General priciples of scanning tunneling optical microscopy, Opt. Lett. ,1989, 14: 1039—1041
19. Pagia H., Radojewski J., and Stotnik N., Operration condition of an optical STM, Optik,1990, 86 (3): 87—90
20. Ohtsu M., Photon Scanning Tunnling Microscope Achieves Nanometer Resolution, Laser Focus World, 1993 (4): News 44
21. Courjon D. and Bainier C., Near-field Microscopy and Near-field Optics,Rep. Prog. Phys., 1994 57: 989—1028
22. The first Photon Scanning Tunneling Microscope has been developed in China, People's Daily News, 1993-06-10 (1) (in Chinese)
23. Guo N., Xia D. K., Wu S. F., Chu S. C., Gao S., Yao J. E., Shang G. Y., and Li C. J., The development of photon scanning tunneling microscopy (PSTM) and its imaging application, Physics, 1993, 22 (12): 679—683 (in Chinese)
24. Wu S. F., Yao J. E., Jian G. S., Guo N., et al., The progress in PSTM, Acta Optica Sinica, 1998, 18 (2): 191—198 (in Chinese)
25. Yao J. E., Wu S. F., Gao S., Guo N., Shang G. Y., Chu S. C., He J., Xia D. K., and Li C. J., Near-field Optical Microscope with nano-meter: PSTM, Journal of Chinese Electron Microscopy Society, 1998, 18 (2): 191—198 (in Chinese)
26. Yao J. E., Gao N., Wu S., Gao S., et al., Photon scanning tunneling microscope and its application, J. Trance Micro-probe Tech., 1997,

15(4): 621—628
27. Wu S. F., Photon Scanning Tunneling Microscope, Now and in the future, Scanning,1995, 17 (1):16—22 (It is an invited paper in The Shanghai First World Optics Congress, Shanghai , 1994, 10)
28. Wu S. F., Jian G. S., and Pan S., How to explain the Image of PSTM, SPIE, 1998, 3467: 34—39
29. Wu S. F., Photo tunneling scanning imaging separating method and instrument, Patent Number: ZL93 1 04111.2, Authorized date: 1999-07-09 (in Chinese)
30. Wu S. F., Photo tunneling scanning imaging separating method and instrument, Japanese Patent Patent Number: 3339658, Authorized date: 2002-08-16 (in Japanese)
31. Wu S. F., Images separating method with AF/PSTM, Patent Number: ZL96 1 11979.9. Authorized date: 2002-07-31 (in Chinese)
32. Wu S. F., Zhang Jiang, Pan Shi, et al., AFM combined with PSTM (AF/PSTM) development, Invited paper on 2002' General Congress of Chinese Optical Society, Changchun, 2002, 9 (in Chinese)
33. Wu S. F., Zhang J., and Pan S., Super resolution Af/PSTM, in: Optics and optical engineering, Beijing: the Publishing House of Science, ISBN 7-3-14760-X, 2004 (in Chinese)
34. Wu S. F., Pan S., and Jian G. S., A comparison between PSTM and A-SNOM, SPIE, 2000, 4098: 125—127
35. Zhang J., Li Y. L., Jian G. S., and Wu S. F., The Advantages of Photon Scanning Tunneling Microscope combined with Atom Force Microscope, Chinese Optics Letters, 2005, 3 (Suppl.): S313—S315
36. Wu S. F, A review of super-resolution of near-field optical imaging, Acta Photonica Sinica, 1998, 27(Z1): 52—54(invited paper)
37. Li Y. L., Wu S. F, Li P. F., et al., Tapping mode atomic force microscope combined with reflection scanning near-field optical microscope (AF/RSNOM), Optics Communications, 2006, 258: 275—279
38. Iwata F., Mikage K., Sakaguchi H., et al., Nanometer scaleelectrochromic modification of NiO films using a novel technique of scanning near-field optical microscopy, Solid State Ionics, 2003, B25, 165: 7—13
39. Vobornik D., Margaritondo G., Sanghera J. S., et al., Spectroscopic infrared scanning near-field optical microscopy (IR-SNOM), Journal of Alloys and Compounds, 2005, 401: 80—88
40. Fragola L., Aigouy P. Y., Mignotte, et al., Apertureless scanning near-field fluorescence microscopy in liquids, Ultramicroscopy, 2004, 101: 47—54
41. Sánchez Erik J., Novotny L, et al., Near-Field Fluorescence Microscopy Based on Two-Photon Excitation with Metal Tips, Physical Review Letters, 1999, 82 (20): 4014—4017
42. Inouye Y., Hayazawa N., Hayashi K., et al., Near-field scanning optical microscope using a metallized cantilever tip for nanospectroscopy, SPIE, 1999, 3791: 40—48
43. Vannier C., Bainier C., and Courjon D., Isotropic incoherent scanning tunneling optical microscope, Optics Communication, 2002, 175: 83—88
44. Jian G. S., Pan S., and Wang Y. G., Simulation of decreasing false image in PSTM with constant scanning mode, Journal of Chinese Electron Microscopy Society, 1998, 8 (1): 15—18 (in Chinese)
45. Wang X. Q., Jian G. S., Wu S. F., Liu W., and Pan S., and A perturbation approach of a multilayer system to the periodic sample for eliminating false image of PSTM, Journal of Chinese Electron Microscopy Society, 2001, 20 (5): 654—657 (in Chinese)
46. Wu S. F., Jian G. S., and Pan S., A survey of nano-meter-resolution near-field optical microscopes, J. of Image and Graphics, 2000, in press (in Chinese)
47. Wu S. F., Jian G. S., and Pan S., How to explain the image of PSTM, SPIE, 1998, 3467: 34—39
48. Wu S. F., Pan S., Liu W., and Wang J. Z., The image separated method with AF/PSTM and its simulated results, Engineering Science, 2001, 3 (8): 33—36 (in Chinese)
49. Jian G. S., Wang J. Z., Wang X. Q., Wu S. F., and Pan S., Using equivalent incident wave method to analysis PSTM, J. of Chinese Electron Microscopy Society, 2003 22 (3): 224—228 (in Chinese)
50. Wang X. Q., Wu S. F., Jian G. S., et al., Simulation of the videotext views of tunneling phenomena of PSTM. Photonelectron and Laser, 2004, 15: 275—278
51. Wang X. Q., Zhang J., Li Y. L., et al., A separation of the refractive index and topography in PSTM: Simulations and experiments, Ultramicroscopy, 2005,104: 1—7
52. Wu S. F., Super-resolution Near-field Optical Imaging and its Industrial Development, Engineering cience,2000, 2 (2): 10—14 (in Chinese)
53. Wu S. F., Jian G. S., Pan S., and Wang Y. G., A measurement of LSF of PSTM imaging with the image of step spread, (Edi) Zhu Xing and Motoichi Ohtsu, Near-field Optics Principles and Applications (IAP-NFO)